The Sphingosine–1–Phosphate (S1P) Lysophospholipid Receptor S1P₃ Regulates MAdCAM-1⁺ Endothelial Cells in Splenic Marginal Sinus Organization

Irute Girkontaite,[1] Vadim Sakk,[1] Martin Wagner,[2] Tilman Borggrefe,[3] Kerry Tedford,[1] Jerold Chun,[4] and Klaus–Dieter Fischer[1]

[1]*Department of Physiological Chemistry,* [2]*Department of Gastroenterology and Endocrinology, and* [3]*Department of Immmunology, University of Ulm, D-89069 Ulm, Germany*

[4]*Department of Molecular Biology, Helen L. Dorris Institute for Neurological and Psychiatric Disorders, The Scripps Research Institute, La Jolla, CA 92037*

Abstract

Marginal zones (MZs) are microdomains in the spleen that contain various types of immune cells, including MZ B cells, MOMA1⁺ metallophilic macrophages, and mucosal addressin cell adhesion molecule 1 (MAdCAM-1)⁺ endothelial cells. MAdCAM-1⁺ and MOMA1⁺ cells line the sinus, that separates MZs from splenic follicles. Here we show that a receptor for the lysophospholipid sphingosine-1-phosphate (S1P), S1P₃, is required for normal numbers of splenic immature and MZ B cells, and for S1P-induced chemotaxis of MZ B cells. S1P₃ is also essential for proper alignment of MOMA1⁺ macrophages and MAdCAM-1⁺ endothelial cells along the marginal sinus. The lack of cohesion of the marginal sinus in S1P₃⁻/⁻ mice affects MZ B cell functions, as wild-type (WT) MZ B cells migrate more into S1P₃⁻/⁻ follicles than into WT follicles after treatment with lipopolysaccharide. Additionally, short-term homing experiments demonstrate that WT MZ B cells home to the S1P₃⁻/⁻ spleen in increased numbers, suggesting a role for the marginal sinus in regulating MZ B cells numbers. Moreover, S1P₃⁻/⁻ mice are defective in mounting immune responses to thymus–independent antigen type 2 due to defects in radiation-resistant cells in the spleen. These data identify lysophospholipids and the S1P₃ receptor as essential regulators of the MZ sinus and its role as a barrier to the follicle.

Key words: marginal zone • B cells • lipopolysaccharide • endothelium • MOMA1⁺ metallophilic macrophages

Introduction

Marginal zones (MZs) are distinct areas in the spleen, defined by the presence of MZ B cells and macrophages, among other cell types, and by their specific location. The MZ forms a layer that envelops a follicle, separating it from the red pulp of the spleen. MZs are bordered on the follicular (FO) side by mucosal addressin cell adhesion molecule 1 (MAdCAM-1)⁺ endothelial cells and by MOMA1⁺ metallophilic macrophages, which line a blood-filled sinus and may regulate entry of blood-borne cells into the follicles (1). MZ B cells react more quickly than FO B cells upon exposure to antigen and are therefore well placed to trigger a rapid response against pathogens such as bacteria carried in the blood because blood channeled into the spleen flows first through MZs (2). The correct localization of MZ B cells in the MZ is governed by factors that include integrin-mediated adhesion to extracellular ligands, attachment to MZ macrophages, expression of the sphingosine-1-phosphate (S1P)₁ receptor, and likely also chemokine-induced MZ B cell migration (3–6). To perpetuate an immune response, MZ B cells move from the MZ into the splenic follicles where T cells, recirculating B cells, and dendritic cells are found. This relocalization can be triggered by antigen, the bacterial endotoxin LPS, or the pharmacological agent

I. Girkontaite and V. Sakk contributed equally to this work.

Address correspondence to Klaus-Dieter Fischer, Dept. of Physiological Chemistry, University of Ulm, Albert-Einstein-Allee 11, D-89069 Ulm, Germany. Phone: 49-731-502-3269; Fax: 49-731-503-1126; email: klaus.fischer@medizin.uni-ulm.de

I. Girkontaite's present address is Fermentas UAB, Graiciuno 8, LT 2028 Vilnius, Lithuania.

FTY720, all of which down-regulate the $S1P_1$ receptor (2, 5–9).

Lysophospholipids, including S1P, are a group of signaling lipids that exert their effects on a wide variety of cell types, including neuronal cells, cardiocytes, cells of the immune system, and endothelial cells (10–13). There are five receptors for S1P, called $S1P_{1-5}$. In vivo studies of mice with mutations in lysophospholipid receptors have revealed wide-ranging roles for the receptors (14). Mice with a mutation of the $S1P_1$ receptor die between days 12.5 and 14.5 due to incomplete vascular formation resulting from defective endothelial cells (15, 16). In chimeric mice lacking $S1P_1$ expression, thymocytes, T cells, and B cells are restricted to lymphoid organs and are unable to circulate freely in blood or lymph fluid (9), whereas MZ B cells are no longer restricted to the MZ but are found inside splenic follicles (5). Thus, $S1P_1$ regulates both endothelial cell organization and lymphocyte localization.

$S1P_3$ receptor knockout mice are viable and exhibit no obvious malformations despite the wide expression of $S1P_3$ in tissues, including heart, lung, kidney, spleen, and thymus (17). However, in $S1P_3$-mutant endothelial cells, high density lipoprotein–induced signaling to calcium fluxing and Akt is defective (18). $S1P_3$, along with $S1P_1$, is also required for directing the organization of endothelial cells into capillary networks (10). Furthermore, $S1P_3$ plays a specific role in MZ B cell migration to S1P in vitro, although it is not required for localization of MZ B cells to the MZ in vivo (5). Additional roles for $S1P_3$ might be compensated for by other S1P receptors, as it was shown that there is redundancy between the $S1P_1$, $S1P_2$, and $S1P_3$ receptors in development of embryonic vascular endothelial cells (19).

In this report, we found that the requirement for $S1P_3$ in MZ B cell migration in vitro did not directly affect MZ B cell localization. Rather, $S1P_3$ was required in vivo for proper arrangement of the MAdCAM-1$^+$ endothelial cells of the marginal sinus and consequently of the MOMA1$^+$ macrophages. The loss of integrity of the marginal sinus meant the loss of a discrete border between MZ B cells and FO B cells and led to defects in MZ functions and immune responses.

Materials and Methods

Mice. 129/Sv WT mice were obtained from Charles River Laboratories. $S1P_3^{-/-}$/LP(B3)/EDG-3$^{-/-}$ mice were generated as described by Ishii et al. (17) and were on a mixed 129/Sv and C57Bl/6 background. Mice used for determining numbers of B cell populations (see Fig. 1) were littermates from interbreedings of $S1P_3^{+/-}$ mice. In all other experiments, age-matched (7–10 wk) mice from interbreedings of $S1P_3^{+/+}$ and $S1P_3^{-/-}$ mice were used. Bone marrow–reconstituted mice were generated by collecting bone marrow cells from WT and $S1P_3^{-/-}$ mice expressing IgM^a by flushing the femur of donor mice with RPMI 1640 medium. 5×10^6 cells were intravenously injected into sublethally irradiated (800 rad) C57B/6 mice (IgM^b) and recipients were analyzed after 6 wk. Complete reconstitution by donor cells was verified by staining splenic B cells for IgM^a and IgM^b expression. B cell chimeric mice were generated by purifying splenic B cells by complement lysis of CD4$^+$ and CD8$^+$ cells followed by Ficoll gradient and intravenously injecting B cells ($1.5–2 \times 10^7$) into RAG-deficient mice. RAG-1$^{-/-}$ mice used were on a C57B/6 background and RAG-2$^{-/-}$ mice that were crossed to $S1P_3^{-/-}$ mice were on a 129/Sv background. LPS injection (15 μg) of mice was performed intravenously (Sigma-Aldrich). All mice were bred and housed in our mouse facility in accordance with institutional guidelines.

Flow Cytometry and Antibodies. Cell surface marker expression was analyzed with a four-color flow cytometer (FACSCalibur; Becton Dickinson) and CELLQuest software using the following antibodies: anti–CD23-PE, anti–B220-PerCP, anti–B220-Cy5, anti–CD21-FITC (BD Biosciences), or purified CD21 biotinylated according to standard protocols and revealed with streptavidin-APC (BD Biosciences).

Migration Assay. Cellular migration was performed in 5-μm pore size Costar transwells essentially as described previously (20). In brief, 10^6 Lympholyte M (Cedarlane)–purified splenocytes were preincubated at 37°C for 0.5–1 h in RPMI 1640 containing 0.25% fatty acid–free BSA (Sigma-Aldrich) and 10 mM Hepes. Cells that had migrated to S1P (Sigma-Aldrich) in the lower chamber were collected after 4 h, stained with anti–CD21-FITC, anti–CD23-PE, and anti–B220-Cy5, and counted with FACSCalibur. MZ B cells were gated as B220$^+$ CD23^{low-} CD21^{hi}. Migration was calculated as a percentage of input.

Immunization. 8-wk-old mice were immunized by intravenous injection of 10 μg TNP-Ficoll. Serum samples were collected before the immunization and at 4 and 8 d after immunization. TNP-specific antibodies were measured by ELISA using plates coated with TNP-BSA. Hapten-specific antibodies were detected with alkaline phosphatase–conjugated antibodies to mouse IgG1, IgG3, and biotinylated antibodies to mouse IgM (all from BD Biosciences). The amount of each antigen-specific isotype was determined by comparing test samples to a standard serum pooled from WT 129/Sv mice and set at 100 arbitrary units (20).

B Cell Homing. Carboxyfluorescein diacetate succinimidyl ester (CFSE; Molecular Probes)–labeled 129/Sv splenocytes were injected intravenously into WT and $S1P_3^{-/-}$ mice (5×10^6 splenocytes/mouse). Recipient mice were killed after 1–1.5 h and the percentage of CFSE$^+$ B cells in spleens was determined by FACS analysis.

Immunofluorescence and Immunohistology. Hematoxylin and eosin stains of 3-μM paraffin sections were performed according to standard protocols. Immunofluorescence staining of 4-μm splenic cryostat sections fixed in acetone was detected using the following antibodies: anti–MOMA1-FITC (Serotec), anti–CD9-biotin revealed by streptavidin-Cy5, anti–MAdCAM-1 followed by anti–rat IgG-biotin revealed by streptavidin-Cy5, anti–IgM-PE, anti–IgD-FITC, and anti–CD1-FITC (BD Biosciences). 10-μm splenic cryostat sections prepared for immunohistology were quenched in 1% H_2O_2 in 40% methanol for 10 min before staining, and stains were revealed with Vectastain Elite ABC peroxidase (Vector Laboratories) and DAB (Vector Laboratories), and counterstained with Methyl Green (Vector Laboratories). Immunofluorescence slides were mounted in Mowiol (Sigma-Aldrich) and immunohistology slides were mounted in Eukitt (Fluka). Slides were analyzed using a Leica DM-IRB microscope and Improvision software (Openlab).

Results

Effects of $S1P_3$ Mutation on Splenic B Cell Subsets. $S1P_3$ is highly expressed in MZ B cells and regulates S1P-induced
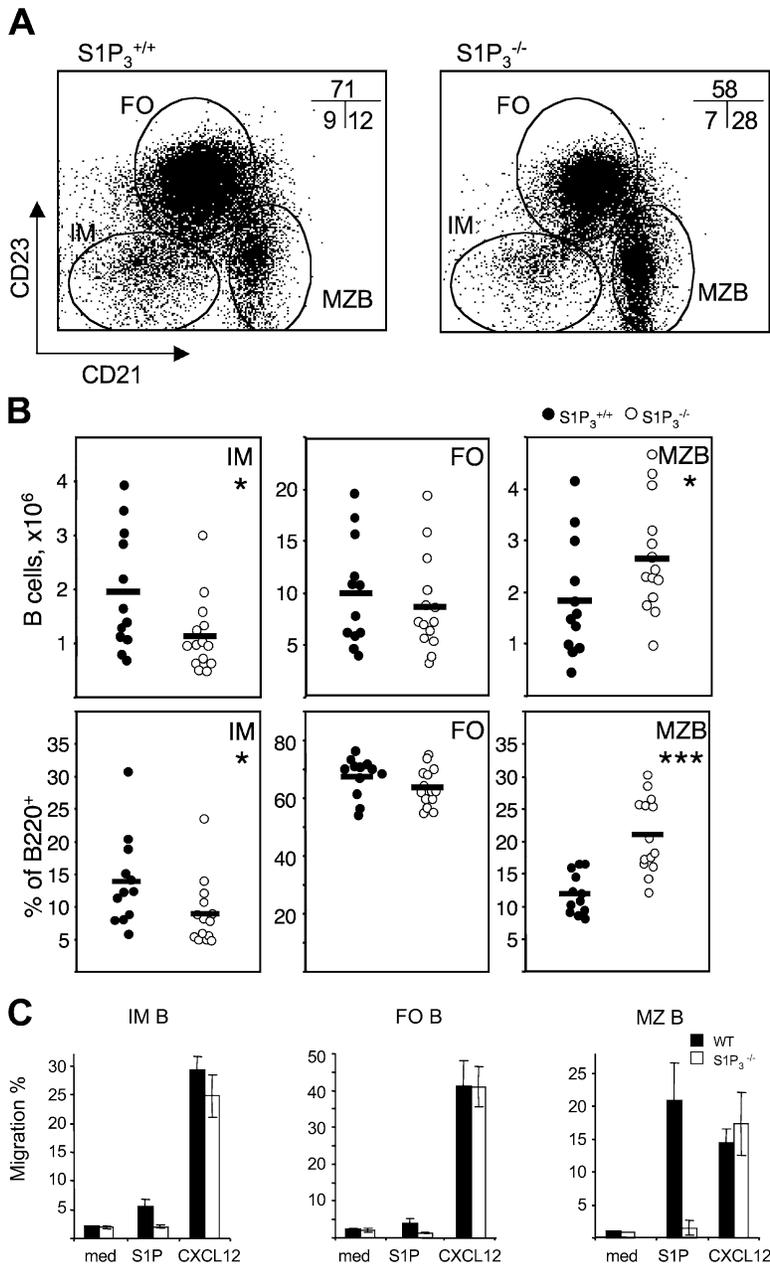
Figure 1. Effects of $S1P_3$ mutation on splenic B cell subsets. (A) FACS analysis of $S1P_3^{+/+}$ and $S1P_3^{-/-}$ splenic B cell populations stained for CD21 and CD23. (B) Absolute numbers (top) and relative numbers (bottom) of splenic B cell populations from $S1P_3^{+/+}$ (●) and $S1P_3^{-/-}$ (○) littermate mice. Statistically significant differences (Student's paired, two-tailed t test) between $S1P_3^{+/+}$ ($n = 12$) and $S1P_3^{-/-}$ mice ($n = 14$) are indicated (*, P < 0.05; ***, P < 0.0005). (C) Migration of splenic B cells in response to medium alone, 0.1 μM S1P, or 0.2 μg/ml CXCL12. Results are the percentage of migration of IM ($B220^+$ $CD23^-$ $CD21^-$), FO ($B220^+$ $CD23^{hi}$ $CD21^{low}$), and MZ ($B220^+$ $CD23^{low-}$ $CD21^{hi}$) B cells to the lower chamber of a transwell from the number of input cells. Bars represent means ± SD ($n = 2$) of at least three experiments.

migration (5). To assess the functions of $S1P_3$ in the splenic MZ, we first evaluated B cell subsets in $S1P_3^{-/-}$ mice. The splenic B cell compartment in mice consists mainly of MZ, FO, and immature (IM) B cells. FACS analysis of splenocytes stained for surface expression of CD21 and CD23 revealed an increase in the size of the MZ B cell compartment (Fig. 1 A). This increase was confirmed by analysis of relative and absolute B cell numbers, which showed an ~40% decrease in IM cells and an increase of ~50% in MZ B cell numbers in $S1P_3^{-/-}$ mice (Fig. 1 B). No significant differences between WT and $S1P_3^{-/-}$ B cell populations in the lymph node and peritoneum were observed (unpublished data). Given the sessile localization of MZ B cells, the increase in MZ B cell numbers prompted us to test $S1P_3^{-/-}$ MZ B cells for the ability to migrate in response to

S1P. As expected, migration of $S1P_3^{-/-}$ MZ B cells was profoundly reduced to S1P (Fig. 1 C). Interestingly, S1P induced migration mainly in MZ B cells and not in FO B cells, although the FO B cell migration still required $S1P_3$ (Fig. 1 C). The basic migration machinery was intact in $S1P_3^{-/-}$ MZ B cells because migration to the chemokine CXCL12 (SDF-1α) was normal (Fig. 1 C). Together, these data show that $S1P_3$ is a regulator of B cell, and in particular of MZ B cell, homeostasis in vivo and that $S1P_3$ is essential for MZ B cell migration in vitro.

Abnormal Splenic Morphology in $S1P_3^{-/-}$ Mice. In light of the role for $S1P_3$ in MZ B cell migration and in endothelial cell organization, we investigated whether the loss of $S1P_3$ affected formation of follicles or the MZ. In hematoxylin and eosin stains of splenic sections from WT mice, the MZ
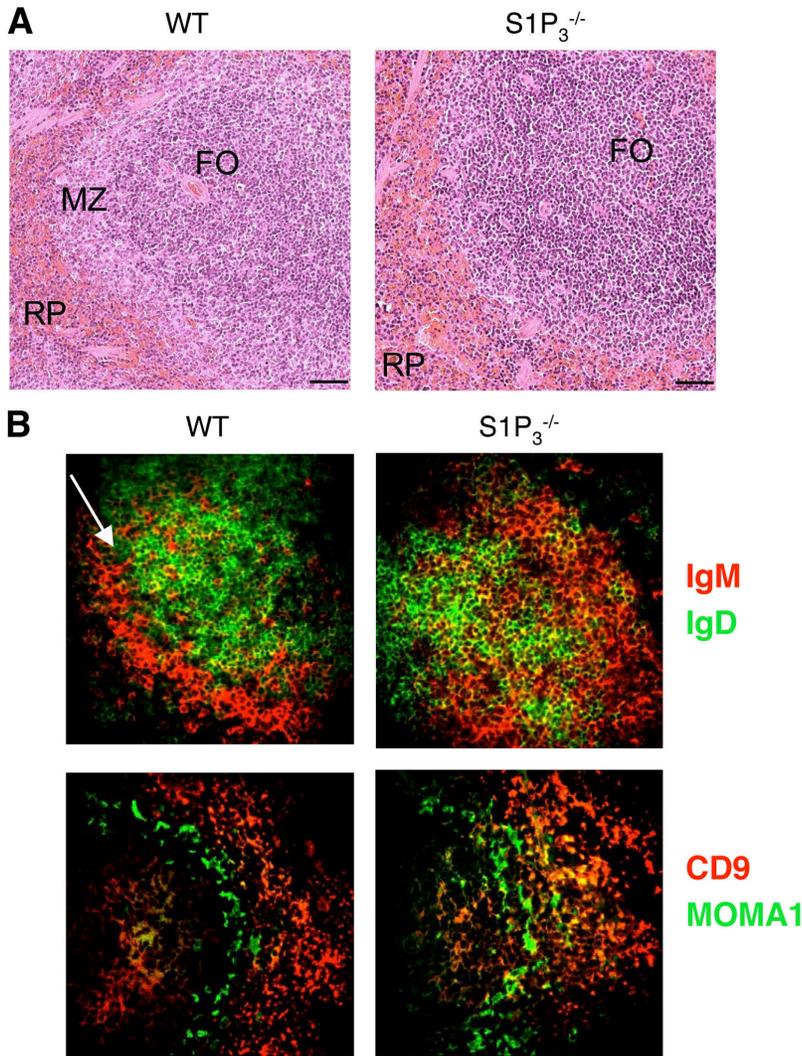
Figure 2. Abnormal MZ morphology in $S1P_3^{-/-}$ mice. (A) Hematoxylin and eosin stains of WT and $S1P_3^{-/-}$ mice with red pulp (RP), follicles (FO), and MZs (MZ) are indicated. Bar, 100 μM. (B) Immunofluorescence analysis of splenic cryosections from WT and $S1P_3^{-/-}$ mice. Sections were stained with anti-IgM (red) and anti-IgD (green), or anti-CD9 (red) and anti-MOMA1 (green). Imaged at a magnification of 40. Arrow in WT section indicates location of marginal sinus. Data are representative of at least five white pulp areas from 5 (A) or 10 (B) each of WT or $S1P_3^{-/-}$ mice.

appeared as a band surrounding a follicle and separating it from the red pulp of the spleen, whereas in $S1P_3^{-/-}$ spleens, the MZ no longer appeared as a defined band (Fig. 2 A). To test the localization of MZ B cells, splenic sections were stained for IgM and IgD. Costaining of splenic sections with IgM and IgD revealed the follicle containing mature FO B cells, which stain highly for IgD, and the MZ containing MZ B cells, which stain highly for IgM. In the absence of $S1P_3$, the MZ was strikingly disordered. Although the bulk of MZ B cells remained in the MZ, increased numbers of IgM^hi cells appeared intermingled with the IgD^hi cells inside the follicle, indicating a loss of organization of the structure of the MZ and of MZ B cells (Fig. 2 B). This was corroborated in a costain of CD9 for MZ B cells (21) and MOMA1^+ metallophic macrophages, which showed MZ B cells extensively interspersed with the MOMA1^+ cells (Fig. 2 B). In WT spleens, the marginal sinus appeared as a thin line where no staining was present, dividing the MZ B cells from the follicle. This line was no longer visible in the disarranged cells of the $S1P_3^{-/-}$ spleen, indicating that the architecture of the marginal sinus was disrupted (Fig. 2 B).

To further characterize the loss of organization in the marginal sinus, splenic sections were stained for MAdCAM-1^+ endothelial cells or for MOMA1^+ metallophilic macrophages. In sections from the WT spleens, the MAdCAM-1^+ cells formed a thin line that encircled the follicles. In sections from $S1P_3^{-/-}$ spleens, the staining of MAdCAM-1^+ cells appeared as a considerably thicker and less defined outline around the follicles (Fig. 3 A). Similarly, cells stained for MOMA1 appeared tightly compressed and almost conjoined in WT spleen sections, but in $S1P_3^{-/-}$ spleen sections, cells were widely spread and appeared to lack cohesion to each other (Fig. 3 A). A view of follicles stained for both MOMA1 and MAdCAM-1 at higher magnification revealed that MOMA1 and MAdCAM-1 were closely colocalized in the WT spleen sections, but not in the $S1P_3^{-/-}$ sections, where cells stained for these markers again appeared to be more widely distributed, discontinuous, and did not colocalize (Fig. 3 B). These findings demonstrate that the lysophospholipid receptor $S1P_3$ is essential for normal arrangement of MAdCAM-1^+ and MOMA1^+ cells lining follicles and for organization of the marginal sinus in the spleen.
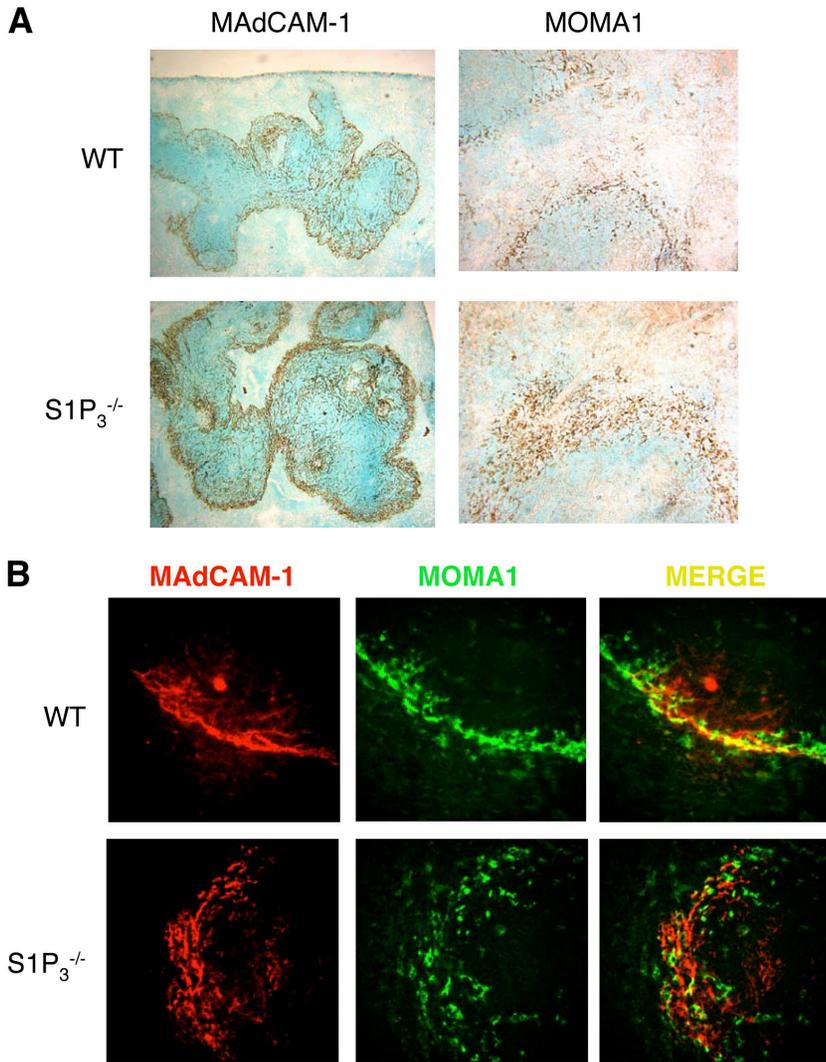
A
MAdCAM-1 MOMA1

WT

S1P$_3^{-/-}$

B
MAdCAM-1 MOMA1 MERGE

WT

S1P$_3^{-/-}$

Figure 3. Disrupted marginal sinus in S1P$_3^{-/-}$ spleens. (A) Immunohistological analysis of MAd-CAM-1 (brown; imaged at a magnification of 10) and MOMA1 (brown; imaged at a magnification of 20) in WT and S1P$_3^{-/-}$ spleen cryosections. (B) Immunofluorescence analysis of splenic cryosections from WT and S1P$_3^{-/-}$ mice stained with anti–MAdCAM-1 (red) and anti-MOMA1 (green; a magnification of 40). On the right, an overlay of left and middle panel images is shown. Data are representative of 5–10 white pulp areas analyzed from at least 5 WT and 5 S1P$_3^{-/-}$ mice per stain.

Disruption of Marginal Sinus Not Caused by S1P$_3^{-/-}$ B Cells. The disruption we observed in the cells lining the marginal sinus could have resulted from a lack of S1P$_3$ in either lymphocytes, particularly MZ B cells, or endothelial cells, among others. To more accurately identify the cell population that caused the defect, we reconstituted RAG-1$^{-/-}$ mice, which lack endogenous lymphocytes, with B cells from either WT or S1P$_3^{-/-}$ mice. In this system, B cells that home to the spleen induce formation of follicles and the expression of MAdCAM-1 in a lymphotoxin-dependent manner (22, 23). In RAG-1$^{-/-}$ mice reconstituted with B cells from either WT or S1P$_3^{-/-}$ mice and analyzed after 14 d, formation of the MAdCAM-1$^+$ and MOMA1$^+$ FO boundary was normal, indicating that S1P$_3^{-/-}$ B cells did not cause faulty organization of MAdCAM-1$^+$ cells (Fig. 4 A). To test the reverse possibility that the defect in S1P$_3^{-/-}$ MAdCAM-1$^+$ cells was intrinsic to the nonlymphoid cells of the spleen, RAG-2$^{-/-}$ mice were crossed to S1P$_3^{-/-}$ mice to generate RAG-2$^{-/-}$ S1P$_3^{-/-}$ double knockout mice. RAG-2$^{-/-}$ and RAG-2$^{-/-}$ S1P$_3^{-/-}$ were then reconstituted with WT B cells. In both cases, MAd-CAM-1$^+$ cells began appearing in an organized, FO-like structure at 8 d after reconstitution. However, the MAd-CAM-1$^+$ FO boundary was thickened and more pronounced in the reconstituted RAG-2$^{-/-}$ S1P$_3^{-/-}$ mice, characteristic of the defect in S1P$_3^{-/-}$ mice (Fig. 4 B, top). These data showed that the defect in S1P$_3^{-/-}$ MAdCAM-1$^+$ cells was not due to failures in the S1P$_3^{-/-}$ MZ B cells to induce the alignment of sinus-forming cells, but rather was endogenous to nonlymphoid cells in the spleen.

Sequential sections from reconstituted RAG-2$^{-/-}$ and RAG-2$^{-/-}$ S1P$_3^{-/-}$ mice were also stained for MOMA1$^+$ macrophages (Fig. 4 B, bottom). Unlike the MAdCAM-1$^+$ cells that appeared in FO shapes at 8 d after reconstitution, MOMA1$^+$ cells formed in a ring-like structure only later after reconstitution and were imaged at day 14, demonstrating that arrangement of the MAdCAM-1$^+$ cells of the marginal sinus precedes that of the MOMA1$^+$ macrophages. Nonetheless, the characteristic S1P$_3^{-/-}$ pattern of disorganization of the MOMA1$^+$ cells was evident in the follicles from RAG-2$^{-/-}$ S1P$_3^{-/-}$ mice (Fig. 4 B, bottom). These data suggest that the disorder in the MOMA1$^+$ cells

A

RAG-1⁻/⁻ + WT   RAG-1⁻/⁻ + S1P₃⁻/⁻

MAdCAM-1

MOMA1

B

8 d.   14 d.

RAG-2⁻/⁻   RAG-2⁻/⁻ S1P₃⁻/⁻   RAG-2⁻/⁻   RAG-2⁻/⁻ S1P₃⁻/⁻
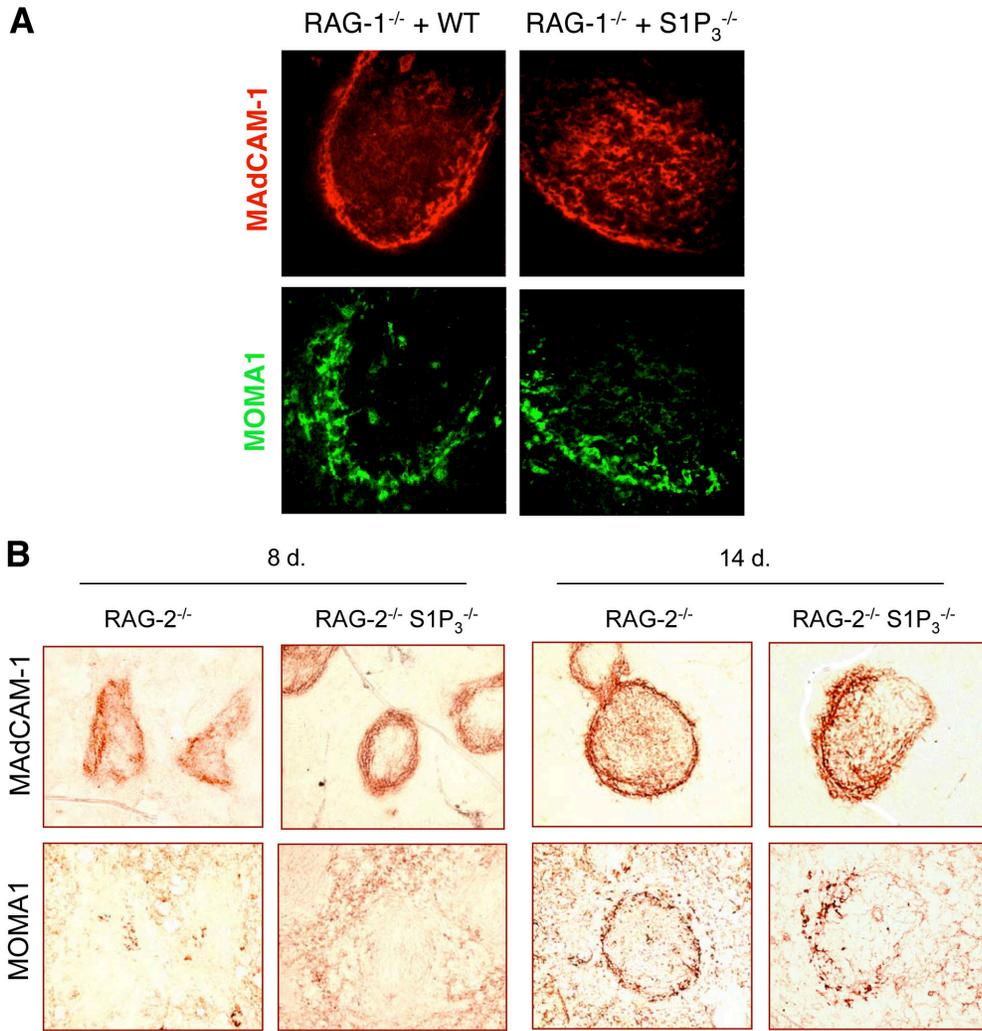
MAdCAM-1

MOMA1

Figure 4. B cells do not cause defective $S1P_3^{-/-}$ marginal sinus. (A) Splenic sections from RAG-$1^{-/-}$ mice 14 d after transfer of splenic B cells from WT and $S1P_3^{-/-}$ mice stained for MAdCAM-1 (red) or MOMA1 (green; imaged at a magnification of 40). Data are representative of at least five white pulp areas analyzed from six RAG-$1^{-/-}$ mice reconstituted either with WT or $S1P_3^{-/-}$ B cells. (B) Splenic sections from RAG-$2^{-/-}$ or RAG-$2^{-/-}$ $S1P_3^{-/-}$ double knockout mice 8 (left) or 14 d (right) after transfer of WT splenic B cells were stained for MAdCAM-1 or MOMA1 (imaged at a magnification of 10). Data are representative of at least four white pulp areas analyzed from two RAG-$1^{-/-}$ and two RAG-$2^{-/-}$ $S1P_3^{-/-}$ recipients per time point.

observed in $S1P_3^{-/-}$ mice was due to the disordered MAd-CAM-1^+ cells.

Increased LPS-induced Entry of MZ B Cells into $S1P_3^{-/-}$ Follicles. MZ B cells respond rapidly to LPS activation by migrating from the MZ into the splenic follicles (2, 6–8). To assess the ability of $S1P_3^{-/-}$ MZ B cells to respond to LPS, splenic sections from WT and $S1P_3^{-/-}$ mice treated with LPS were stained both for CD1 as a marker of MZ B cells (24, 25) and for MAdCAM-1 to define the border between the MZ and the follicle. Over a 3-h time course, a greater proportion of $S1P_3^{-/-}$ MZ B cells appeared within follicles outlined by MAdCAM-1 staining compared with WT (Fig. 5 A). Thus, either $S1P_3^{-/-}$ MZ B cells are inherently faster than WT at migrating to LPS, or the disorganized structure of the $S1P_3^{-/-}$ MZ enables either genotype of MZ B cells to get to the follicle faster than the WT MZ does. To distinguish between these possibilities, we reconstituted irradiated mice with either WT or $S1P_3^{-/-}$ bone marrow and then tested them for LPS-induced MZ B cell migration. FO entry was similar in WT mice reconstituted with either WT or $S1P_3^{-/-}$ bone marrow (Fig. 5 B), thus the increased rate of entry of $S1P_3^{-/-}$ MZ B cells shown in

Fig. 5 A was not intrinsic to the MZ B cells. In the reverse case, when $S1P_3^{-/-}$ mice reconstituted with WT bone marrow were treated with LPS, the proportion of MZ B cells apparent within the follicle was relatively increased (Fig. 5 B). Therefore, activated MZ B cells are able to traverse the disorganized $S1P_3^{-/-}$ MZ more rapidly than a WT MZ, resulting in a more complete level of FO entry.

Increased Homing of MZ B Cells to $S1P_3^{-/-}$ Spleens. To determine if the disorganization of the $S1P_3^{-/-}$ MZ influenced the ability of lymphocytes to home to the spleen, we performed a short-term homing experiment using WT splenocytes as donor cells and WT or $S1P_3^{-/-}$ mice as recipients. Equal numbers of splenocytes pooled from WT mice were labeled with CFSE and transferred to WT or $S1P_3^{-/-}$ recipients. FACS analysis was performed on splenocytes from the recipients 90 min after injection of the labeled donor cells to determine the relative numbers of CFSE-labeled cells (Fig. 6 A). Donor WT IM and FO B cells were found in similar numbers in WT and $S1P_3^{-/-}$ recipient spleens. However, twofold more WT MZ B cells homed to the $S1P_3^{-/-}$ recipient spleen than to the WT spleen, suggesting that the $S1P_3^{-/-}$ spleen MZ niche permitted increased numbers of MZ B cells
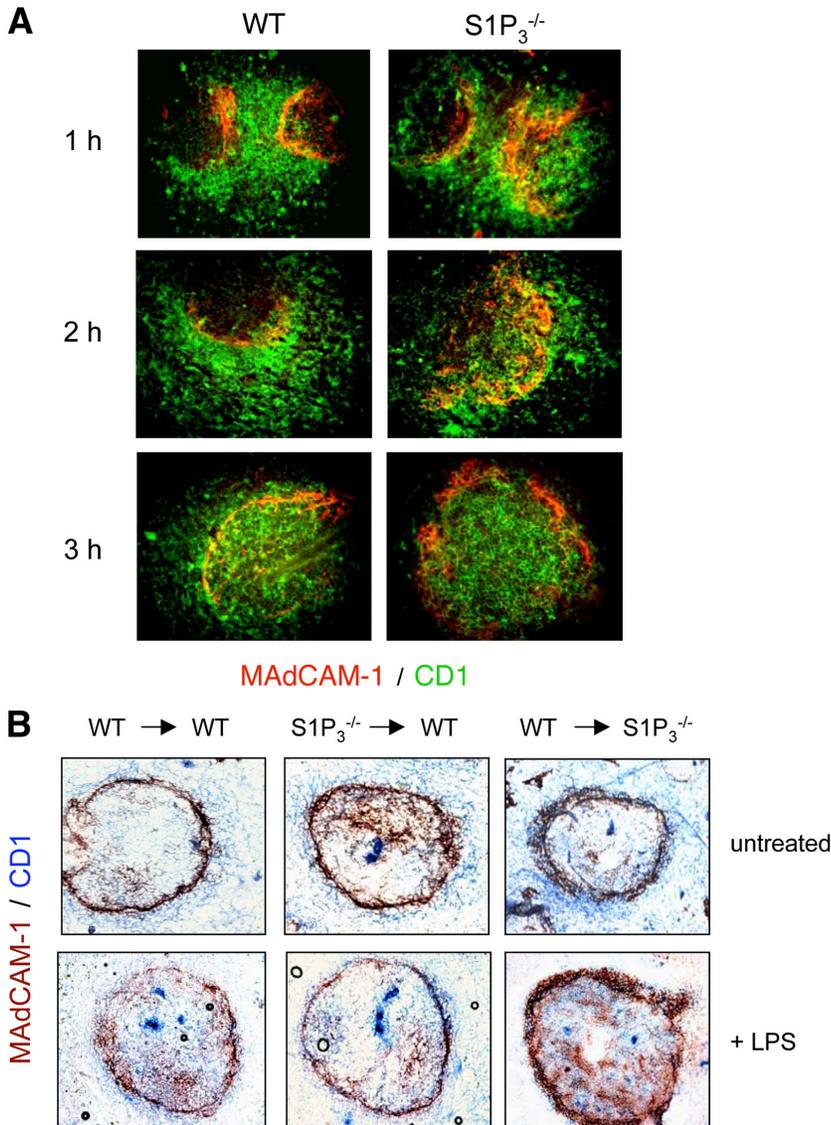
A

WT   S1P₃⁻/⁻

1 h

2 h

3 h

MAdCAM-1 / CD1

B

WT → WT   S1P₃⁻/⁻ → WT   WT → S1P₃⁻/⁻

MAdCAM-1 / CD1

untreated

+ LPS

Figure 5. Faster FO entry of LPS-treated MZ B cells in S1P₃⁻/⁻ spleens. (A) WT and S1P₃⁻/⁻ mice were treated with 15 μg LPS and spleens were isolated at the indicated time points (in hours). Splenic sections from treated mice were stained for CD1 (green) to identify MZ B cells or for MAdCAM-1 (red) to mark boundary of marginal sinus and follicles (imaged at a magnification of 40). Data are representative of 5–10 white pulp areas analyzed from 3 WT and 3 S1P₃⁻/⁻ mice per time point. (B) Irradiated WT or S1P₃⁻/⁻ mice reconstituted with either WT or S1P₃⁻/⁻ bone marrow as indicated were treated with PBS as a control or 15 μg LPS. Immunohistochemical sections were prepared from spleens isolated 2 h after treatment and stained for CD1 (blue) and MAdCAM-1 (brown; imaged at a magnification of 20). Data are representative of at least 5–10 white pulp areas analyzed from at least 3 WT and S1P₃⁻/⁻ mice per group.

(Fig. 6, A and B). The experiment was repeated with lymph node B cells to determine if the increased numbers of MZ B cells in S1P₃⁻/⁻ spleens was due to the acquisition of MZ B cell markers by other types of B cells, but no MZ B cells were detected, showing that conversion was not the source of the increased MZ B cells (unpublished data). This finding indicated that the S1P₃⁻/⁻ spleen supported only normal numbers of IM and FO B cells, but enabled increased numbers of MZ B cells in the spleen, most likely because of the localized disarrangement of MZ sinuses in S1P₃⁻/⁻ spleens.

Defective Immune Responses in S1P₃⁻/⁻ Mice. MZ B cells are substantial contributors to the rapid thymus–independent (TI) immune response (26). To assess the strength of TI-2 immune responses in S1P₃⁻/⁻ mice, serum levels of IgM, IgG1, and IgG3 were measured at defined time points after intravenous immunization with TNP-Ficoll. A significant decrease in IgM levels was observed in S1P₃⁻/⁻ mice 4 d after immunization. Similarly, a significant decrease in IgG3 levels was also observed 8 d after immunization (Fig.

7 A). These data demonstrate that a receptor for lysopholipids, S1P₃, is required to achieve a full immune response.

These defective immune responses suggested that the S1P₃⁻/⁻ MZ B cells were unable to fully respond to antigen. To test whether the S1P₃⁻/⁻ MZ B cells were indeed responsible, we tested immune responses in chimeric mice generated from irradiated WT mice reconstituted with S1P₃⁻/⁻ bone marrow (Fig. 7 B). Surprisingly, immune responses to TI-2 antigen were normal in these mice. This finding indicated that the defects observed in the immune responses from the nonreconstituted mice (Fig. 7 A) were not intrinsic to lymphoid or radiation-sensitive cells, but rather to radiation-resistant cells in the spleen, and imply that the splenic architecture is important for proper lymphocyte function.

Discussion

The MZ that surrounds lymphocyte follicles in the spleen acts as a protective border for the follicle. It contains the
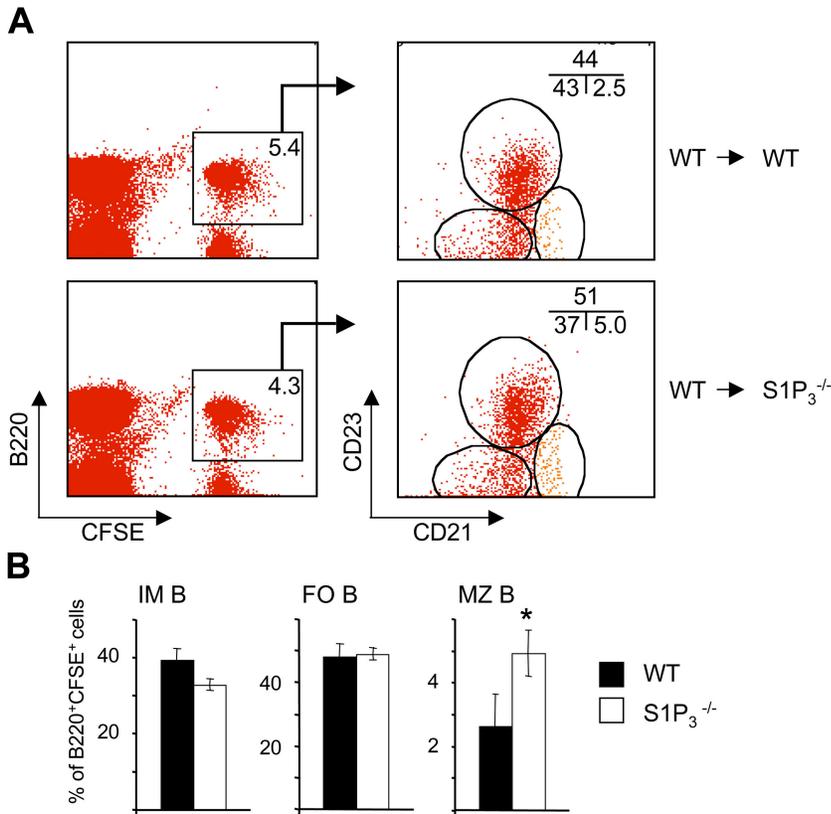
Figure 6. Increased homing of WT MZ B cells to $S1P_3^{-/-}$ spleen. (A) Representative flow cytometry plot of 5×10^6 CFSE-labeled splenocytes from WT 129/Sv mice injected intravenously into WT or $S1P_3^{-/-}$ mice. Splenocytes were obtained from mice after 1–1.5 h and stained with anti–CD23-PE, anti–B220-PerCP, and anti–CD21-biotin and streptavidin-APC. The percentage of CFSE-labeled IM ($B220^+$ $CD23^-$ $CD21^-$), FO ($B220^+$ $CD23^{hi}$ $CD21^{low}$), and MZ ($B220^+$ $CD23^{low-}$ $CD21^{hi}$) B cells was calculated from total numbers of $B220^+$ $CFSE^+$ cells. (B) Bar graphs show means ± SD for 20-wk-old WT (black bars; $n = 3$) and $S1P_3^{-/-}$ mice (white bars; $n = 3$) representative of two independent experiments. Statistically significant differences (Student's paired, two-tailed t test) are indicated (*, $P < 0.05$).

marginal sinus, which includes MAdCAM-1$^+$ endothelial cells in a relatively tight formation surrounding the follicle. It is also exposed to circulating blood. Therefore, the cells in the MZ are able to sample blood for dangerous pathogens or for growth or chemotactic factors. In this report, we show that the S1P receptor, $S1P_3$, regulates diverse functions in various MZ cells types. In chemotactic assays, $S1P_3$ is required for MZ B cell migration to S1P. In vivo, $S1P_3$ is essential for the cohesion and organized arrangement of MAdCAM-1$^+$ and MOMA1$^+$ cells along the splenic marginal sinus. In addition, $S1P_3^{-/-}$ mice have slightly decreased numbers of IM B cells and increased numbers of MZ B cells.

MZ B cells migrate strongly to S1P, which is present in relatively high concentrations in blood serum. We and others have shown that the critical receptor for S1P-induced migration is $S1P_3$, but this role for $S1P_3$ is specific to MZ B cells because S1P activates only minimal migration in FO B cells (5). Intriguingly, the $S1P_1$ receptor is not a strong regulator of MZ B cell migration in vitro, as is $S1P_3$; however, $S1P_1$-mutant MZ B cells are mislocalized and are found inside follicles and not in the MZ (5). In contrast, despite the essential role for $S1P_3$ in MZ B cell migration to S1P in vitro, MZ B cells were still present in the MZs of $S1P_3^{-/-}$ splenic follicles in vivo. Thus, S1P-induced migration is not required for initially locating MZ B cells in the MZ, but may serve some other function that we have not been able to measure. For example, one possibility would be that during a particular type of immune response such as a T cell–dependent response, FO dendritic cells secrete S1P to attract MZ B cells.

Although MZ B cells were present in the MZ of $S1P_3^{-/-}$ mice, they appeared disordered and interspersed with the MAdCAM-1$^+$ cells that line the marginal sinus. In WT spleens, the MAdCAM-1$^+$ cells were tightly cohesive and present in a thin layer encircling the follicles, and MZ B cells appeared in a broad ring that encircled the MAdCAM-1 cells and the marginal sinus, but that was separate from the follicles. In contrast, in $S1P_3^{-/-}$ spleens, MAdCAM-1$^+$ cells were discontinuous and widely spread, and MZ B cells were no longer distinct from the endothelial layer. Using B cell reconstitution of mice, we demonstrated that the mislocalization of MZ B cells was not intrinsic to B cells but to radiation-resistant cells in the spleen, which would include the MAdCAM-1$^+$ endothelial cells. Thus, the lack of migration to S1P by $S1P_3^{-/-}$ MZ B cells in vitro was not responsible for this in vivo defect. S1P affects many functions in endothelial cells (10, 27) and $S1P_1$ is essential to endothelial cell organization into networks (15, 16). Therefore, the defects in marginal sinus organization in $S1P_3^{-/-}$ mice may result from endothelial cells that are unable to respond to S1P, and that cannot use $S1P_1$ or $S1P_2$ to compensate for loss of $S1P_3$. The level of expression of $S1P_3$ on endothelial cells of the marginal sinus is currently unknown due to the lack of antibodies against $S1P_3$ and to difficulty in isolating the endothelial cell population for RT-PCR assessment of expression levels.

Supporting the idea that defects in organization of the $S1P_3^{-/-}$ MZ are due to endothelial cell failures, it was reported that inhibition of $S1P_1$ and $S1P_3$ expression in
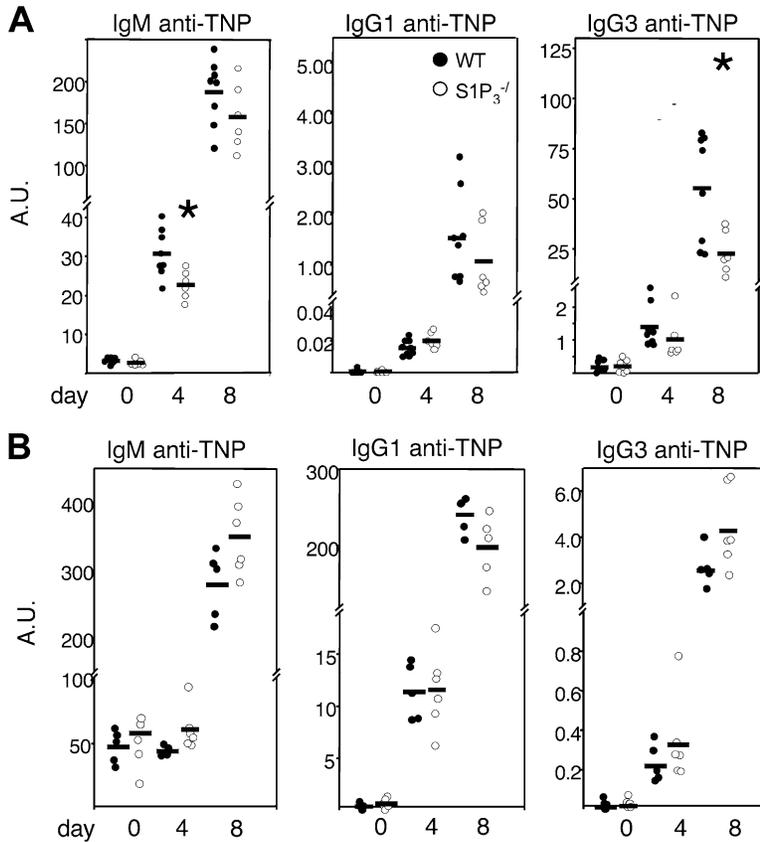
Figure 7. Defective immune responses to TI-2 antigen in $S1P_3^{-/-}$ mice are not dependent on lymphoid cells. (A) WT ($n = 8$) and $S1P_3^{-/-}$ ($n = 6$) mice were immunized with TNP-Ficoll, a TI-2 antigen, and primary immune responses in arbitrary units (A.U.) were assessed on days 4 and 8. Asterisks denote significant differences ($P < 0.05$; Student's paired, two-tailed t-test) between WT and $S1P_3^{-/-}$ mice. (B) Immune responses to TNP-Ficoll were assessed in chimeric mice composed of irradiated, WT mice reconstituted with either WT or $S1P_3^{-/-}$ bone marrow. Primary immune responses were assessed on days 4 and 8 in WT to WT chimeras (●; $n = 8$) or $S1P_3^{-/-}$ to WT chimeras (○; $n = 8$). No statistically significant differences were observed.

HUVEC cells results in a disordered endothelial cell layer, as S1P activates Rho GTPases and actin assembly upstream of VE-cadherin clustering and adherens junction assembly (10). Moreover, $S1P_3^{-/-}$ endothelial cells are defective in high density lipoprotein-induced signaling, vasodilation, and arterial blood pressure (18). In the spleen, MAdCAM-1^+ endothelial cells appear to regulate FO entry and lymphocyte homing (1, 28); therefore, the disrupted marginal sinus in $S1P_3^{-/-}$ mice may translate into a functional defect. In agreement with this possibility, we found that LPS-activated MZ B cells in $S1P_3^{-/-}$ spleens migrate more into follicles than WT MZ B cells. Using chimeric mice, we showed that this enhanced migration was not due to the $S1P_3^{-/-}$ MZ B cells, but rather to radiation-resistant cells in the spleen, such as endothelial cells. Therefore, it is likely that this augmented migration to LPS is due to the lack of an intact marginal sinus because the endothelial cells might no longer form a border regulating access of activated cells to the follicle.

Both MAdCAM-1^+ endothelial cells and MOMA1$^+$ macrophages are disordered in $S1P_3^{-/-}$ marginal sinus. We demonstrated that MAdCAM-1^+ cells are the source of the primary defect because their formation into FO ring-like structures precedes that of MOMA1$^+$ cells. Moreover, data from NKX2.3, RelB, and op/op mice support the idea that MAdCAM-1^+ expression on cells precedes the appearance of MOMA1$^+$ cells (29–31). These findings suggest the possibility that MAdCAM-1^+ cells secrete a chemoattractant

that acts on the MOMA1$^+$ cells in the formation of the marginal sinus. In addition, the disorganized MOMA1$^+$ macrophages may contribute to the defects in MZ functions we observed, such as the reduction in immune responses to TI-2 antigen in $S1P_3^{-/-}$ mice. TI antigens stimulate MZ B cells to activate an immune response (26). However, the defective immune responses were not due to defects in MZ B cells or other radiation-sensitive cells because $S1P_3^{-/-}$ bone marrow–reconstituted WT mice had normal immune responses. Therefore, the integrity of the MZ is probably key to immunity to antigens that depend on MZ B cells. Although mutations in NKX2.3 and RelB lead to loss of MAdCAM-1 expression on splenic cells (29–31), to our knowledge, only mutation of $S1P_3$ leads to defective organization of MAdCAM-1^+ cells in the spleen.

In short-term homing experiments, WT MZ B cells were found in increased numbers in $S1P_3^{-/-}$ spleens. These findings suggested that the disordered MAdCAM-1^+ cell layer in $S1P_3^{-/-}$ spleens contributed to the increased MZ B cell retention. Thus, the increased numbers of MZ B cells we observed in $S1P_3^{-/-}$ mice might be due to the disordered endothelium in the MZ. If the cells of the MZ are no longer constrained by the barrier of the marginal sinus and can infiltrate the follicle, then the factors that ensure retention of MZ B cells in the MZ would have greater amounts of space and could therefore trap larger numbers of MZ B cells. This increase in the niche size for MZ B cells might allow the development of greater numbers of

MZ B cells, possibly due to increased contact with MAd-CAM-1, MOMA1^{+}, or other cells in the MZ. Conversely, numbers of MZ B cells were normal in WT mice reconstituted with S1P$_3$[−/−] bone marrow (unpublished data), supporting the idea that the increase in numbers of S1P$_3$[−/−] MZ B cells was not a defect inherent to the MZ B cells. The decreased numbers of IM B cells in the spleen, in contrast to the increased MZ B cell numbers, might be due to decreases in numbers of S1P$_3$[−/−] bone marrow B cells (unpublished data).

Although S1P$_1$, S1P$_2$, and S1P$_3$ have overlapping functions in embryogenesis (19), analysis of mice with individual mutations in these receptors has revealed specific roles for them in immunity. For example, S1P$_1$ regulates T and B cell exit from lymphoid organs as well as MZ B retention in the MZ (5, 9). Here we report on a specific function for S1P$_3$ in the organization of MAdCAM-1^{+} endothelial cells surrounding splenic follicles and show that immune functions including FO entry, size of MZ niche, and immune responses are defective in this context. These results indicate that the MAdCAM-1^{+} cells serve as a barrier to the follicle and regulate immunity, possibly by preventing unregulated access to FO cells. S1P$_3$ may regulate this barrier by ensuring tight contacts between endothelial cells, as it does in embryonic vascular maturation. This understanding of S1P$_3$ may assist in the design of immunotherapies to control lymphocyte activation and circulation, such as FTY720, targeted at S1P receptors and signaling.

References

1. Kraal, G., K. Schornagel, P.R. Streeter, B. Holzmann, and E.C. Butcher. 1995. Expression of the mucosal vascular addressin, MAdCAM-1, on sinus-lining cells in the spleen. *Am. J. Pathol.* 147:763–771.
2. Martin, F., and J.F. Kearney. 2002. Marginal-zone B cells. *Nat. Rev. Immunol.* 2:323–335.
3. Guinamard, R., M. Okigaki, J. Schlessinger, and J.V. Ravetch. 2000. Absence of marginal zone B cells in Pyk-2-deficient mice defines their role in the humoral response. *Nat. Immunol.* 1:31–36.
4. Karlsson, M.C., R. Guinamard, S. Bolland, M. Sankala, R.M. Steinman, and J.V. Ravetch. 2003. Macrophages control the retention and trafficking of B lymphocytes in the splenic marginal zone. *J. Exp. Med.* 198:333–340.
5. Cinamon, G., M. Matloubian, M.J. Lesneski, Y. Xu, C. Low, T. Lu, R.L. Proia, and J.G. Cyster. 2004. Sphingosine
6. Lu, T.T., and J.G. Cyster. 2002. Integrin-mediated long-term B cell retention in the splenic marginal zone. *Science.* 297:409–412.
7. Groeneveld, P.H., T. Erich, and G. Kraal. 1985. In vivo effects of LPS on B lymphocyte subpopulations. Migration of marginal zone-lymphocytes and IgD-blast formation in the mouse spleen. *Immunobiology.* 170:402–411.
8. Kraal, G. 1992. Cells in the marginal zone of the spleen. *Int. Rev. Cytol.* 132:31–74.
9. Matloubian, M., C.G. Lo, G. Cinamon, M.J. Lesneski, Y. Xu, V. Brinkmann, M.L. Allende, R.L. Proia, and J.G. Cyster. 2004. Lymphocyte egress from thymus and peripheral lymphoid organs is dependent on S1P receptor 1. *Nature.* 427:355–360.
10. Lee, M.J., S. Thangada, K.P. Claffey, N. Ancellin, C.H. Liu, M. Kluk, M. Volpi, R.I. Sha'afi, and T. Hla. 1999. Vascular endothelial cell adherens junction assembly and morphogenesis induced by sphingosine-1-phosphate. *Cell.* 99:301–312.
11. Le, L.Q., J.H. Kabarowski, Z. Weng, A.B. Satterthwaite, E.T. Harvill, E.R. Jensen, J.F. Miller, and O.N. Witte. 2001. Mice lacking the orphan G protein-coupled receptor G2A develop a late-onset autoimmune syndrome. *Immunity.* 14:561–571.
12. Fukushima, N., I. Ishii, J.J. Contos, J.A. Weiner, and J. Chun. 2001. Lysophospholipid receptors. *Annu. Rev. Pharmacol. Toxicol.* 41:507–534.
13. Lauber, K., E. Bohn, S.M. Krober, Y.J. Xiao, S.G. Blumenthal, R.K. Lindemann, P. Marini, C. Wiedig, A. Zobywalski, S. Baksh, et al. 2003. Apoptotic cells induce migration of phagocytes via caspase-3-mediated release of a lipid attraction signal. *Cell.* 113:717–730.
14. Ishii, I., N. Fukushima, X. Ye, and J. Chun. 2004. Lysophospholipid receptors: signaling and biology. *Annu. Rev. Biochem.* 73:321–354.
15. Liu, Y., R. Wada, T. Yamashita, Y. Mi, C.X. Deng, J.P. Hobson, H.M. Rosenfeldt, V.E. Nava, S.S. Chae, M.J. Lee, et al. 2000. Edg-1, the G protein-coupled receptor for sphingosine-1-phosphate, is essential for vascular maturation. *J. Clin. Invest.* 106:951–961.
16. Allende, M.L., T. Yamashita, and R.L. Proia. 2003. G-protein coupled receptor S1P1 acts within endothelial cells to regulate vascular maturation. *Blood.* 102:3665–3667.
17. Ishii, I., B. Friedman, X. Ye, S. Kawamura, C. McGiffert, J.J. Contos, M.A. Kingsbury, G. Zhang, J.H. Brown, and J. Chun. 2001. Selective loss of sphingosine 1-phosphate signaling with no obvious phenotypic abnormality in mice lacking its G protein-coupled receptor, LP(B3)/EDG-3. *J. Biol. Chem.* 276:33697–33704.
18. Nofer, J.R., M. van der Giet, M. Tolle, I. Wolinska, K. von Wnuck Lipinski, H.A. Baba, U.J. Tietge, A. Godecke, I. Ishii, B. Kleuser, et al. 2004. HDL induces NO-dependent vasorelaxation via the lysophospholipid receptor S1P3. *J. Clin. Invest.* 113:569–581.
19. Kono, M., Y. Mi, Y. Liu, T. Sasaki, M.L. Allende, Y.P. Wu, T. Yamashita, and R.L. Proia. 2004. S1P1, S1P2, and S1P3 receptors coordinately function during embryonic angiogenesis. *J. Biol. Chem.* 279:29367–29373.
20. Girkontaite, I., K. Missy, V. Sakk, A. Harenberg, K. Tedford, T. Potzel, K. Pfeffer, and K.D. Fischer. 2001. Lsc is required for marginal zone B cells, regulation of lymphocyte motility and immune responses. *Nat. Immunol.* 2:855–862.

21. Won, W.J., and J.F. Kearney. 2002. CD9 is a unique marker for marginal zone B cells, B1 cells, and plasma cells in mice. *J. Immunol.* 168:5605–5611.

22. Crowley, M.T., C.R. Reilly, and D. Lo. 1999. Influence of lymphocytes on the presence and organization of dendritic cell subsets in the spleen. *J. Immunol.* 163:4894–4900.

23. Tumanov, A., D. Kuprash, M. Lagarkova, S. Grivennikov, K. Abe, A. Shakhov, L. Drutskaya, C. Stewart, A. Chervonsky, and S. Nedospasov. 2002. Distinct role of surface lymphotoxin expressed by B cells in the organization of secondary lymphoid tissues. *Immunity.* 17:239–250.

24. Amano, M., N. Baumgarth, M.D. Dick, L. Brossay, M. Kronenberg, L.A. Herzenberg, and S. Strober. 1998. CD1 expression defines subsets of follicular and marginal zone B cells in the spleen: beta 2-microglobulin-dependent and independent forms. *J. Immunol.* 161:1710–1717.

25. Roark, J.H., S.H. Park, J. Jayawardena, U. Kavita, M. Shannon, and A. Bendelac. 1998. CD1.1 expression by mouse antigen-presenting cells and marginal zone B cells. *J. Immunol.* 160:3121–3127.

26. Martin, F., A.M. Oliver, and J.F. Kearney. 2001. Marginal zone and B1 B cells unite in the early response against T–independent blood-borne particulate antigens. *Immunity.* 14:617–629.

27. Spiegel, S., and S. Milstien. 2003. Sphingosine-1-phosphate: an enigmatic signalling lipid. *Nat. Rev. Mol. Cell Biol.* 4:397–407.

28. Tanaka, H., Y. Hataba, S. Saito, O. Fukushima, and M. Miyasaka. 1996. Phenotypic characteristics and significance of reticular meshwork surrounding splenic white pulp of mice. *J. Electron Microsc. (Tokyo).* 45:407–416.

29. Pabst, O., R. Forster, M. Lipp, H. Engel, and H.H. Arnold. 2000. NKX2.3 is required for MAdCAM-1 expression and homing of lymphocytes in spleen and mucosa-associated lymphoid tissue. *EMBO J.* 19:2015–2023.

30. Weih, D.S., Z.B. Yilmaz, and F. Weih. 2001. Essential role of RelB in germinal center and marginal zone formation and proper expression of homing chemokines. *J. Immunol.* 167:1909–1919.

31. Pasparakis, M., S. Kousteni, J. Peschon, and G. Kollias. 2000. Tumor necrosis factor and the p55TNF receptor are required for optimal development of the marginal sinus and for migration of follicular dendritic cell precursors into splenic follicles. *Cell. Immunol.* 201:33–41.